Lab on a Chip

PAPER

View Article Online
View Journal | View Issue

Cite this: *Lab Chip*, 2020, **20**, 2020

Capacitive sensing of triglyceride film reactions: a proof-of-concept demonstration for sensing in simulated duodenal contents with gastrointestinal targeting capsule system†

George E. Banis, [ab] Luke A. Beardslee,[a] Justin M. Stine,[ac] Rajendra Mayavan Sathyam[ac] and Reza Ghodssi*[abc]

Received 10th February 2020,
Accepted 26th April 2020

DOI: 10.1039/d0lc00133c

rsc.li/loc

Ingestible capsule systems continue to evolve to overcome drawbacks associated with traditional gastrointestinal (GI) diagnostic and therapeutic processes, such as limitations on which sections of the GI tract can be accessed or the inability to measure local biomarker concentrations. We report an integrated capsule sensing system, utilizing a hybrid packaging scheme coupled with triglyceride film-coated capacitive sensors, for measuring biochemical species present in the duodenum, such as pancreatic lipase and bile acids. The system uses microfabricated capacitive sensors interfaced with a Bluetooth low-energy (BLE)-microcontroller, allowing wireless connectivity to a mobile app. The triglyceride films insulate the sensor surface and react either with 0.01–1 mM lipase *via* hydrolysis or 0.07–7% w/v bile acids *via* emulsification in simulated fluids, leading to measurable changes in capacitance. Cross reactivity of the triglyceride films is evaluated in both phosphate buffered saline (PBS) as well as pancreatic trypsin solutions. The film morphology is observed after exposure to each stimulus to better understand how these changes alter the sensor capacitance. The capsule utilizes a 3D-printed package coated with polymers that remain intact in acid solution (mimicking gastric conditions), then dissolve at a duodenum-mimicking neutral pH for triggered opening of the sensing chamber from which we can subsequently detect the presence of pancreatic lipase. This device strategy represents a significant step towards using embedded packaging and triglyceride-based materials to target specific regions of the GI tract and sensing biochemical contents for evaluating gastrointestinal health.

Introduction

Ingestible capsule systems capable of navigating the gastrointestinal (GI) tract are being developed to non-invasively address a myriad of clinical applications.[1–4] The most recognizable device is the capsule endoscope, such as the PillCam (Medtronic, Dublin, Ireland), EndoCapsule (Olympus, Tokyo, Japan), and MiroCam (IntroMedic Co., Seoul, South Korea), which can visualize the entire GI tract length, but are most useful for imaging the small intestine where access *via* traditional endoscopic techniques remains limited.[5–8] Capsules directed toward monitoring specific GI analytes have been developed to provide more specific diagnostic information than is available with video imaging. For example, a capsule containing sensors targeting various gases, specifically H_2, CH_4, and CO_2, has been demonstrated for profiling gas content within porcine and human GI tracts and to the effects of various stimuli such as heat stress, anti-inflammatory agents, high- and low-fiber diets.[9–12] There are also capsules measuring a variety of parameters including: pH, temperature, or pressure, as well as cancer markers using near-infrared sensors to measure fluorescently tagged antibodies. Integrated capsule systems have also been designed that enhance drug delivery through programmable control systems or controlled release.[13,14] Several capsules have been developed to detect GI bleeding using either fluorometric sensors to measure circulating fluorophores or photodetectors measuring heme-triggered light emitted from engineered bacteria.[15–19] Though they are measuring similar contents, the electronic architecture-based on their respective transduction mechanisms – and materials chosen vary, requiring differences in fabrication and integration strategies.[20] For the GI bleeding capsules, one requires

[a] *Institute for Systems Research, University of Maryland, USA. E-mail: ghodssi@umd.edu*
[b] *Fischell Department of Bioengineering, University of Maryland, USA*
[c] *Department of Electrical and Computer Engineering, University of Maryland, College Park, MD, USA*

† Electronic supplementary information (ESI) available. See DOI: 10.1039/d0lc00133c

intravenous application of the fluorophores while the other utilizes embedded bacteria. In comparing the gas- or pH-detecting capsules, the phase or state of the detected medium varies, demanding transducers adaptable for measuring contents whether they are in gas or liquid form, both of which are present in the GI environment.[21]

Recent advances in fabrication methods allowing the integration of a broader range of materials have fostered the development of more capsule devices. 3D-printing, one of the most ubiquitous and continuously expanding manufacturing technologies, has improved the time, cost efficiency, and allowable structural complexity for device prototyping compared to traditional subtractive manufacturing processes.[22] Increased spatial resolution enables 3D-printing of microfluidics and microsystems packaging, while research for 3D-printed biocompatible materials has led to implementation into medical and pharmaceutical devices.[22–26] Further, food-based materials, including varieties of gelatin, starches, or oils, are increasingly becoming utilized for edible electronic systems.[27–30] Integration of these materials on sensors, either as electrodes or as electrode-functionalized substrates, have allowed for catalyzing reactions directly with target analytes; however, fabrication and integration challenges vary significantly, depending on the chemical composition of the material, and have yet to find utility in capsule devices.[31]

This paper presents an integrated capsule system that utilizes biocompatible and biodegradable materials as packaging for GI-targeted fluid sampling, and triglyceride films for sensing digestive enzymes in a target region. Polymers that dissolve in a specific pH range are used as the packaging materials and are able to target fluids with characteristics simulating pancreatic secretions due to their characteristic pH. The pH gradient of the GI tract is relatively well understood, with the gastric – or stomach – environment known to be highly acidic (pH 1–3),[32] though can occasionally increase outside this range with different feeding or fasting states.[33] Gastric secretions flowing into the duodenum are then neutralized by bicarbonate secretions entering *via* the sphincter of Oddi from the pancreas (pH 5–7). Therefore, systems and sensors entering the stomach must be well protected to remain stable upon entry into the small intestine. A previously developed packaging strategy is utilized in which biodegradable polymers, such as various Eudragit formulations, allow fluid to enter the capsule at specific locations within the GI tract.[34] The Eudragit L100 formulation is pH-specific and dissolves above pH 6.0 but remains stable in lower pH levels, protecting the sensing chamber until the capsule reaches the duodenum.[35–37] A target molecule of interest is pancreatic lipase (PL), which is known to diminish in response to a variety of pancreatic pathologies such as exocrine pancreatic insufficiency, cystic fibrosis, pancreatitis, and even pancreatic cancer.[38–42] Current methods for elaborating PL activity consist of blood, urine, or stool tests, which generally require admission to a hospital or clinic, potential blood withdrawal, and lab analysis.[43] A user-friendly device capable of point-of-care (POC) PL measurements would reduce the time to reach diagnosis measurements and cost for patients suffering from chronic pancreatic conditions, which require frequent sampling and analysis.[44] Lipase serves additionally as a model target – for more specific enzymes or other biomolecules that are present only in specific regions of the GI tract – for detection with the targeting capsule system presented here.

Here, stearin was used as a model substrate for measuring PL activity in a capacitive-sensing capsule system that is designed to specifically sample pancreatic secretions in the duodenum. The attractive nature of the sensors is their utility for measuring film solubility in a capsule package, which can be applied to a variety of targets analytes that induce film- or substrate-dissolving reactions. A similar sensing strategy for measuring pancreatic trypsin with films made from gelatin is previously reported.[28] Testing of the sensors consisted of observing the sensor response over time frames similar to those expected while traveling through the duodenum, while immersed in varying concentrations of pancreatic lipase in a benchtop environment that reflect a similar expected range with appropriate pH.

In using this strategy, the impact of bile acids (BA) were investigated, as they were identified as a probable interfering species. BAs are synthesized from cholesterol by hepatocytes; they are shown to be elevated in GI secretions during BA malabsorption and can be further related to conditions such as irritable bowel syndrome-associated diarrhea and colorectal cancer.[45–47] Because of their amphipathic nature, BAs such as cholic and deoxycholic acid act as natural detergents that emulsify triglycerides to form micelles through intercalation, aiding their digestion by PL into absorbable monoglycerides and fatty acids.[48] The system was characterized by testing stearin films with BAs to determine potential nonspecific impacts and how it may affect sensing of PL, then further characterize its integration into a capsule platform with the downstream goal of wirelessly transmitting metrics of these biochemical species to a patient for potential clinical evaluation.

Fig. 1 Illustrates the prospective data flow from the capsule sensor to the patient's physician. The system is potentially low-cost, biocompatible, and easily interfaces with a mobile phone for wirelessly collecting data *via* Bluetooth low energy (BLE). The system offers promise for further development of ingestible diagnostic systems that would benefit from novel integration and packaging strategies for measuring biomarkers, such as enzymes, in GI secretions.

Materials and methods

A. Description of device, operation, and data acquisition

The capsules were designed and assembled at the University of Maryland, College Park. The capsule shell is 3D-printed with MED610, a biocompatible resin, using an Objet500 Connex3 (Stratasys, Rehovot, Israel). The printed circuit board (PCB) and electronic components, were commercially manufactured (Sunstone, Mulino, OR) and assembled

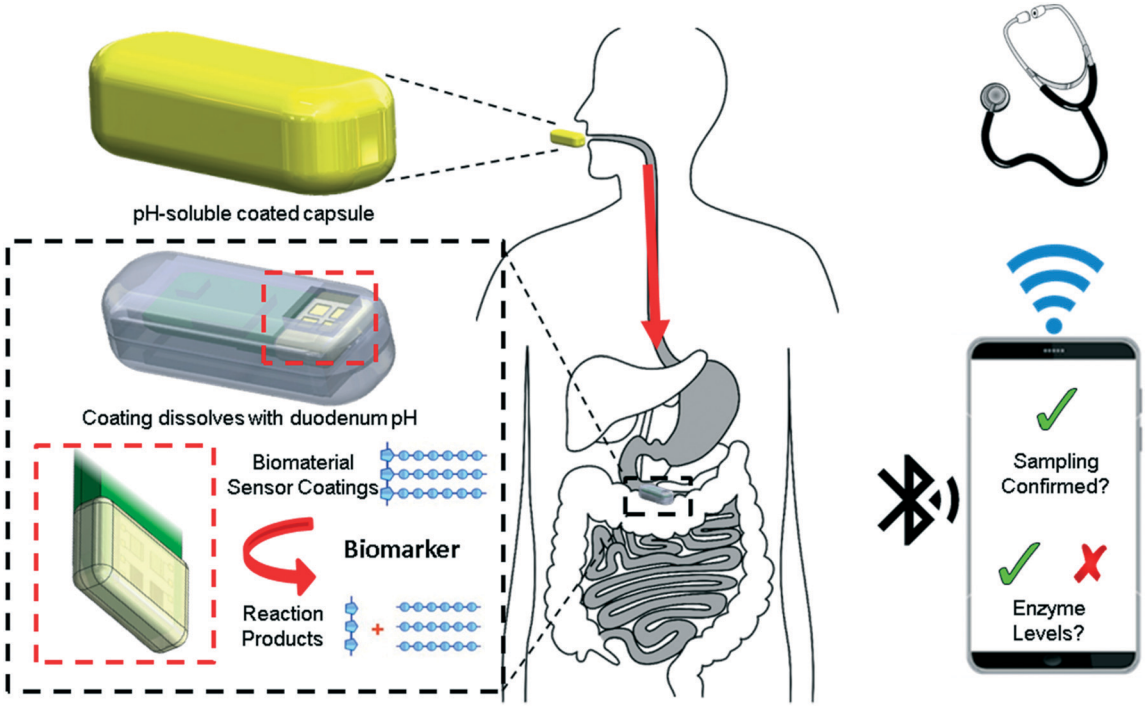

Fig. 1 Depiction of application. The pH-soluble coated capsule is ingested and protected from acidic pH, reflecting that of the stomach, until reaching the small intestine. Upon dissolution, the fluid is sampled *via* embedded gratings, and pancreatic lipase reacts with triglyceride coatings to increase the capacitance of the sensors. The signal is transmitted to a phone wirelessly and shared with a medical practitioner.

(Screaming Circuits, Canby, OR). Specifications for the system electronics and capsule dimensions are presented in Table 1, while a detailed method describing the capsule assembly is discussed in ESI† Fig. S1. The capacitive sensors consist of interdigitated electrodes, described previously, capped with plasma-enhanced chemical vapor deposited 100 nm SiO_2 films.[49] Fig. 2 depicts photographs of the sensor PCB assembly (SPA), and the subsequent encapsulation in the capsule shell. In commentary of the capsule dimensions, the current largest capsule standard size is 000, which measures at 9.9 mm × 26.1 mm, whereas the dimensions of the clinically utilized InteliSite capsule (Innovative Devices, LLC, Raleigh, North Carolina, USA) measures at 10 mm × 35 mm, indicating larger capsules may still be usable for certain populations.[50] Efforts to reduce dimensions are continuously in development to reduce potential for affecting GI motility, while more discussion on current capsule dimensions can be found in other studies.[4]

Table 1 System specifications

3D-printed shell	
Outer diameter	12.7 mm
Inner diameter	11.5 mm
Length	35 mm
Inlet area	4 mm^2
Sensors	
Finger width	5 μm
Finger spacing	5 μm
Finger length	750 μm
Number of fingers	80
Finger thickness	200/20 Au/Cr nm
Electronics	
PCB length	25.8 mm
PCB width	10.4 mm
Sensor capacitance range	0.8–220 pF
Sensor capacitance sensitivity	7.3 pF mV^{-1}
Operating voltage	3.3/5.0 V (component dependent)
Current consumption	Active/deep sleep: 5 mA/2.5 μA
Battery (powerstream)	Li-Polymer/14 mA h/3.7 V
Wireless communication	BLE 2.4 GHz

The SPA was powered at 3.3 V and paired to a nearby Android phone *via* BLE through a custom application. To operate the device, a signal was transmitted from the phone to trigger the SPA to enter deep sleep mode (2.5 μA) for 2.5 hour, allowing for material deposition processes to be completed. Following the deep sleep duration, the SPA entered active mode (~5 mA), the app would request a capacitance value from the microcontroller with a sampling rate of 1 Hz. The data is timestamped and stored into a matrix, which could be uploaded to the cloud after each experiment and downloaded to a PC. The data was then visualized for analysis with a MATLAB GUI.

B. Deposition of film and coating materials

The sensing mechanism is based on the enzymatic and physicochemical reactions presented in Fig. 3, which features

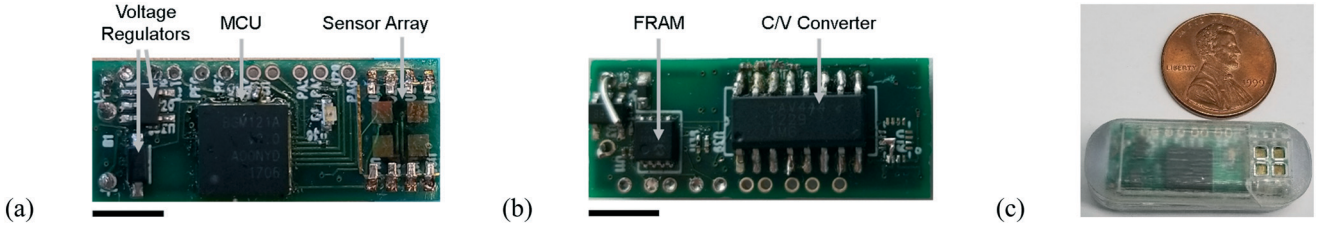

Fig. 2 (a) Top and (b) bottom views of sensor PCB assembly (SPA), and (c) photograph of assembled capsule. Scale bar = 5 mm.

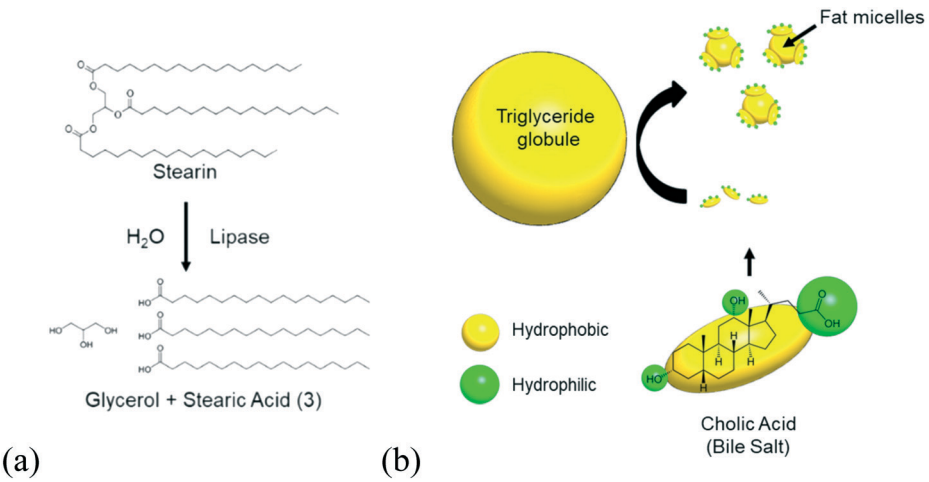

Fig. 3 (a) Lipase-induced hydrolytic digestion of stearin into glycerol and three stearic acid molecules. (b) Bile salt-induced emulsification of triglyceride globules into micelles.

(a) the hydrolysis of triglyceride ester linkages by PL and (b) the emulsification of triglyceride globules by BAs. Stearin was used as a model triglyceride due to its high melting point (54–72.5 °C) to remain stable at physiological temperature (37–39 °C).[51] The triglyceride solution was prepared for coating onto the sensor surface and consisted of a mixture of stearin and glycerol, where several stearin : glycerol (SG) ratios were evaluated. The combinations included stearin, 2 : 1, 1 : 1, and 1 : 2 ratios of SG after allowing the suspension to melt in a 100 °C water bath prior to deposition. Multiple film deposition strategies were investigated, as depicted in ESI† Fig. S2. Drop-casting and dip-coating of molten SG solution, while the substrates were either left at ambient or pre-heated for 5 minutes to SG melting temperature, were compared. In evaluating overall stability and uniformity, the films used for testing PL and BA were deposited *via* dip-coating of the SPAs, depicted in Fig. 4a. The SPAs were pre-heated for 5 minutes to above substrate melting temperature (~100 °C), then immersed and subsequently removed The films were air cooled at ambient temperature, forming SG-coated SPAs (SG-SPAs), and the resulting thicknesses were measured using calipers.

The SG-SPAs were inserted into the capsule *via* the assembly process described in ESI† Fig. S1, and the capsules were subsequently dip-coated into a dyed pH-sensitive copolymer

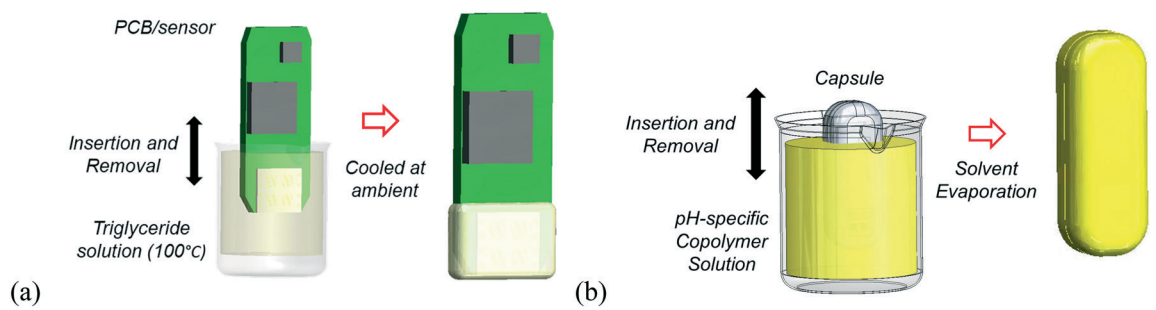

Fig. 4 (a) Dip-coating of pre-heated PCB/sensor assemblies into triglyceride solution for film formation. (b) Dip-coating of assembled capsules into dyed pH-sensitive copolymer solutions to form GI-targeting coatings, repeated for sequential coatings.

solution, depicted in Fig. 4b. The copolymer solution utilized for this study was 30% Eudragit L100 in methanol, producing coatings 783 ± 60 μm thick using a previously described coating process.[49] After coating, capsules were stored between 24 and 48 hours before experiments at ambient temperature (~23–24 °C), though storage at different temperatures may affect coating stability over time.

C. Sensing characterization

SG-SPA characterization was performed while powered by an Agilent E3631A DC power supply (Santa Clara, CA). For the SG-SPAs prepared in section B, each experiment was initiated with baseline measurements while the device was suspended in air. After 5 minutes, the devices were lowered into a 50 mL beaker containing solutions of either negative control – *i.e.* buffer only – then subsequent test conditions, described below. All buffer solutions consisted of 40 mL of 0.1 M phosphate buffered saline (PBS) on a hot plate set to 300 RPM stir *via* magnetic stir bar to equilibrate the solution and temperature at 39 °C. All solutions were prepared using deionized water from E-pure ultrapure water purification systems (DI H_2O; resistivity = 18.0 Ω cm; Thermo Scientific, Waltham, MA).

The sensor capacitance response was determined for each analyte in an environment that simulated fluids present in the duodenum. SG-SPAs were immersed in pH 7.3 buffer containing varying concentrations of either porcine PL or a BA mixture of sodium cholate and sodium deoxycholate (Sigma Aldrich, St. Louis, MO). PL was tested at 1 mM, 100 μM, and 10 μM concentrations, while BA was tested across 175, 17.5, and 1.75 mM, equivalent to 7, 0.7, and 0.07% w/v. To measure potential impact of nonspecific enzymes, porcine pancreatic trypsin (Sigma) was also tested alone at 100 μM, a concentration that exceeds maximum expected outputs by >250%.[52] Each solution was incubated for 30 minutes at 39 °C prior to insertion into a beaker for testing the SG-SPAs to ensure complete solubility.

D. SEM analysis for film morphology

Pre-heated sensor die were inserted into molten 2 : 1 SG solution prepared as described in section B. The sensors were then cooled at ambient (23 °C) for 24 hours, then incubated in glass petri dishes containing PBS (0.1 M) alone or with either 100 μM PL, 0.7% w/v BA or 100 μM trypsin, respectively. Each solution was maintained at 39 °C under 300 rpm stir. Sensors were removed from solution after either 30 or 60 minutes, rinsed with DI H_2O, dried for 24 hours, then prepared in a carbon coater to deposit coatings of conductive carbon (MED 010 Balzers Union Carbon Coater, Balzers Union, Liechtenstein). The samples were then viewed under a Hitachi S-3400 scanning electron microscope (SEM).

E. pH-Dependent sampling and sensing

Following a similar procedure as in section C, measurements were performed while suspending the coated capsule in air, then subsequently inserted into a test solution. For these experiments, the electronics were powered by a Li-polymer battery (Powerstream, West Orem, Utah). The capsules were inserted for a duration of 25 min into several solutions, which mimicked the pH transition between the stomach (acidic) and duodenum (neutral), as depicted in Fig. 5. The solutions consisted of the following conditions: (i) 0.1 M acetic acid (pH 3), (ii) PBS (pH 7.3), and (iii) 1 mM PL in PBS (pH 7.3). This sequence was chosen to reflect the capsule transit throughout the GI tract with the subsequent presence of a specific biomarker residing in the ESI,† in this case PL.

Results and discussion

This work presents a sensing strategy using triglyceride films to detect duodenal contents, such as lipase and bile acids, in a wireless capacitive-sensing platform. The sensors were designed to measure the capacitive response when fluid enters the sensing chamber. Under biological stimuli from species in the environment, the substrate films deposited over the sensors undergo hydrolysis or emulsification reactions that alter their dielectric property. Gradually, the dissolution of the film substrate exposes the electrode fingers to the infiltrating fluid, causing an increase in capacitance. The sensor capacitance was measured for SG-SPAs and coated capsules inserted into various solutions containing

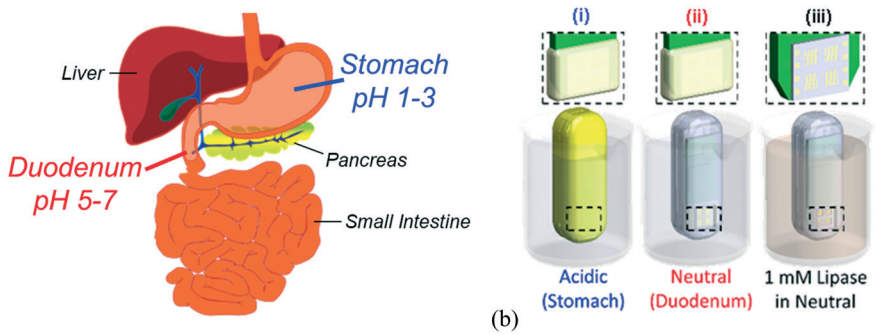

Fig. 5 (a) Schematic depicting normal GI pH progression along with adjacent organs. (b) Experimental setup for complete capsule characterization.

biochemical stimuli, described in C and E, which induce changes in capacitance over different lengths of time when compared to non-specific controls or buffer alone.

Stearin was the material chosen as our model triglyceride, as described in B. The digestion of triglycerides, is enabled by emulsion and subsequent hydrolysis by BAs and PL, respectively. Due to its rigidity and low water solubility – an effect of having longer chain fatty acids – unmodified stearin is an inefficient substrate for hydrolysis. Other triglycerides such as oleic acid – a shorter chain fatty acid found in olive oil – are used as standard substrate for lipase assays; however, these substrates are incompatible with our system function in the small intestine due to having a melting point below physiological temperature.[53] Previous reports modify stearin as a substrate using suspensions with glycerol by enhancing the quality of the interface it would have with lipase.[54–56] Lipase activity on triglycerides is generally dependent on the surface area, which increases significantly with rougher surfaces or when emulsified into micelles by BAs. While crystalline stearin films are naturally hydrophobic, glycerol is hydrophilic due to polar –OH groups, enhancing the interface between the species in solution and the film substrate, as well as a stable film deposition and adhesion over the sensor surfaces.

Because the platform has demonstrated utility for monitoring changes in sensor capacitance (C), the dielectric properties of the films can be described through estimation by eqn (1):

$$C = \frac{2\varepsilon_r\varepsilon_0 lwn}{d} = \frac{\varepsilon_r\varepsilon_0 A}{d} \quad (1)$$

Here, ε_0 (vacuum permittivity), ε_r (dielectric constant), l (finger length), w (finger width), n (numbers of electrode fingers), and d (distance of separation), where $2lwn$ can be simplified to A (total area of both electrodes). Therefore, cumulative changes in the dielectric properties and thickness of the films are proportional to measured capacitance (C) and indicate the extent of hydrolysis or emulsification of the substrate over the sensor. To account for changes in baseline capacitance between experiments, the sensor response as the percent change in capacitance (%ΔC) can be calculated with eqn (2):

$$\%\Delta C = \left(\frac{C_n - C_1}{C_1}\right) \times 100 \quad (2)$$

Here, C_n is the capacitance at n sample in time, where C_1 is the capacitance at the beginning of the recorded sequence such as those presented in Fig. 6.

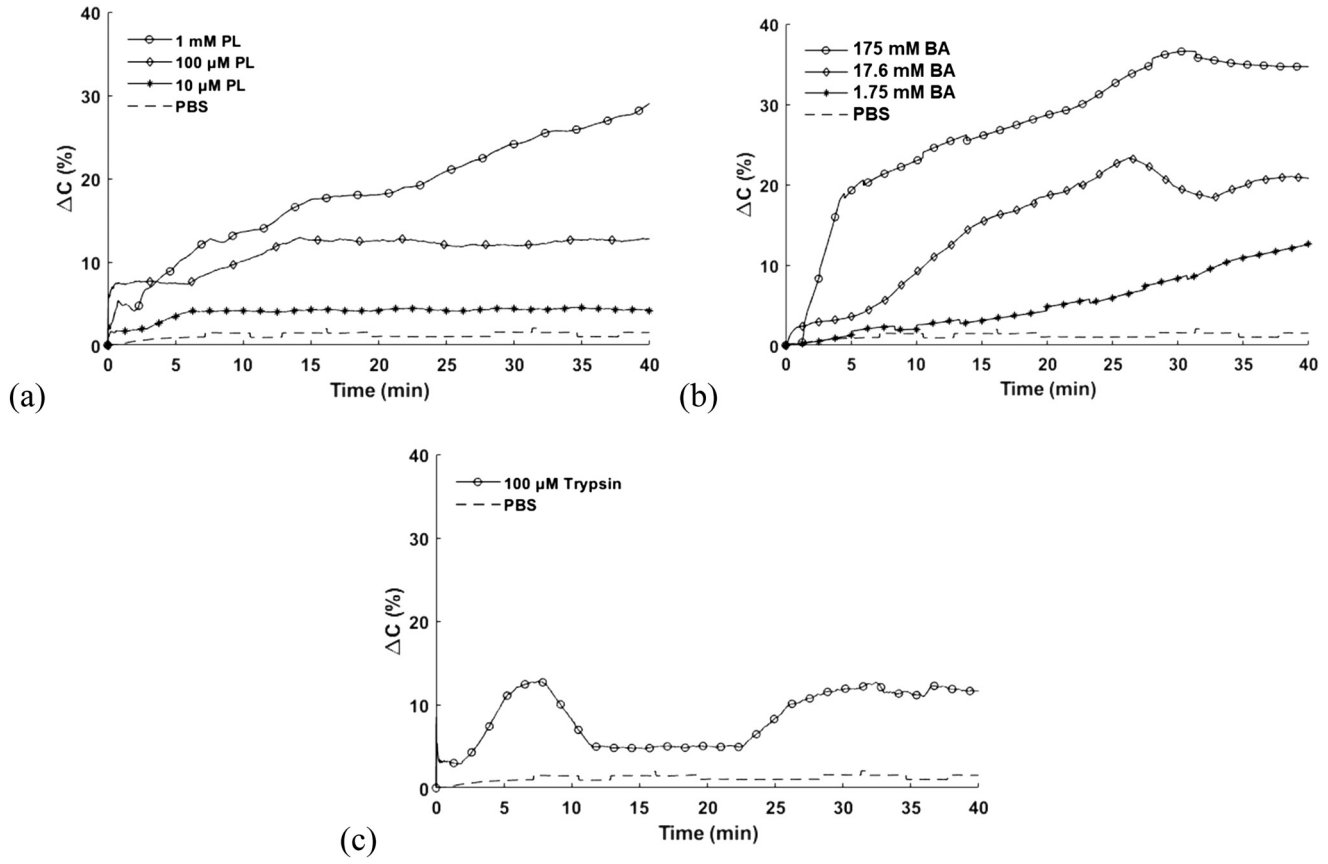

Fig. 6 Sensing in the presence of different biochemical species at varying concentrations compared to PBS alone. (a) PL at 10 μM, 100 μM, and 1 mM, (b) BAs at 1.75, 17.5, and 175 mM, and (c) pancreatic trypsin at 100 μM.

When no film is present – *i.e.* one of our negative controls – and the sensor is inserted into PBS, the mean $\%\Delta C$ is 39.5 ± 1.4, likely a resulting effect of the higher dielectric constant of water as compared to air combined with ionic reactions with the SiO_2 films, which can be mitigated in the future through more inert films.[57] As expected, insertion into molten and cooled SG solutions produced negligible $\%\Delta C$, indicating that changes in capacitance are limited to (when the dielectric properties of the SG material is influenced by an environmental condition – such as the applied solutions and constituent analytes described in *C*.

Initial tests consisted of the effect of different deposition strategies of the SG solutions onto the sensors, described in section B. Substrate temperature was considered a significant factor due to its effect on surface tension, and therefore wetting of the solution.[58] In the case of drop-casting, three phases (*i.e.* solid, liquid, gas) are present at the sensor surface during the entirety of the process, thus surface tension becomes a more dominant factor for wetting, and therefore coating, the sensors. Wetting through dip-coating, however, causes most of the sensor surface (except for the edges) to be exposed to only two phases with the ability for a complete wetting and sealing layer, reducing the dependency on surface tension. Additionally, the order of the wetting transition has a direct impact on the adsorbed film thickness, such that the greater the discontinuity in the interfacial energy between phases, the greater the thickness. This discontinuity is reflected by the difference in temperature between the substrate and film, which were observed through thinner films produced when the substrates are pre-heated. SiO_2 films on the sensor surfaces are generally hydrophilic, with surface energies of ~73.8 mJ m^{-2}, compared to most triglycerides, which maintain surface energies ranging from 25–30 mJ m^{-2} as reported in the literature; this increases with temperature as well, producing further discontinuity and, therefore, wetting angle.[59,60] Adhesion between the SiO_2 and SG layers is primarily based on van der Waals interactions; however, the drop-cast films were found to not be stable, as the films did not produce an adequate enough seal at the substrate surface and failed to prevent buffer from interacting with the sensors (data not shown).[61] After comparing the efficacy of the film deposition methods, SG-SPAs were tested using films produced through pre-heating the substrate to 100 °C and dip-coating, which yielded an average film thickness of 210 ± 60.3 μm. The total sensor area was 0.06 mm^2, indicating each film volume over the sensors to be 1.25×10^{-5} cm^3. In comparing the sensor response for different SG film compositions (see C), the 2 : 1 SG ratio films were found to be most stable when in buffer alone (ESI† Fig. S3), hence their implementation in the following sensor characterization experiments. From the 2 : 1 SG ratio, the volume of stearin contained within the film was calculated to be 0.84×10^{-5} cm^3, and with a density of 0.862 g cm^{-3}, the stearin mass was found to be 0.724×10^{-5} g, or 8.12×10^{-9} mol (molecular weight of stearin: 891.5 g mol^{-1}).

The standard concentration of PL expected in healthy unstimulated duodenal fluid ranges from 1–10 μM.[62] Conversely, average duodenal secretions contain 0.7% w/v BA, which reflects the median concentration tested in this work.[63] Because PL is dependent on BAs for improving the enzyme–substrate interface with triglycerides, it was necessary to determine the individual effect of both species on the dielectric properties of the film, which can range from characteristics such as ratio of stearic acid to glycerol *via* hydrolysis, stearin to glycerol through emulsion separation, or even overall SG film to solution contact with the sensor surface. Fig. 6 presents the capacitive response ($\%\Delta C$) of the SG-SPA over time upon immediate insertion into the solution at t = 0 minutes, where the concentration of the biological stimuli was varied for PL (0.01–1 mM) and BAs (1.75–175 mM), as well as pancreatic trypsin (100 μM) to measure potential nonspecific interactions. Each sequence begins directly following insertion of the SG-SPA into the test solution to precede experiments of the sensors within a capsule device. Measurements were compared to a buffer-only solution (7.3 pH, PBS) as a negative control. The capacitance responses of films to both PL and BAs produced trends that altered proportionally to the concentration of the analytes present. Conversely, the signal for trypsin did not produce consistent trends, and appeared to experience stabilizing transients throughout the time frame of the experiments; the effect of trypsin at different concentrations requires further investigation. The measurement was conducted over the course of 40 minutes, consistent with the expected transit time of most contents passing through the duodenum, though longer time scales have been reported.[64] Additionally, nonspecific activity testing with extracted duodenal secretions and its regular contents will be necessary for increasing confidence in sensor specificity, though stearin appears to be a resilient insulator to negative controls. To modify the system for response to lower concentrations, it is likely that parameters such as concentration of substrate at the sensor surface or film thickness will need to be reduced such that the dielectric properties of the film can change faster. This is consistent with our findings where films exceeding 200 μm thickness produced no significant change in capacitance compared to buffer alone (data not shown), indicating that either increasing film thickness may reduce reactivity or penetration of the enzyme or that the film is too thick to see a measurable effect over the experimental time period, requiring more film removal before observing a change in capacitance. Reducing the film thickness would be feasible through closer matching of the surface energies, such as through temperature or surface tension, between the SPAs and SG solution before dip-coating, as well as dissolving the triglyceride in nonpolar solvents such as ethers, hexane, or chloroform in lower concentrations.[29,65]

After measuring the capacitive response to each concentration, the slopes were used as a metric to fit the sensitivity. Fig. 7 presents calibration curves comparing the slope of the capacitive response for the first 30 minutes of sampling ($\%\Delta C/\Delta t$) compared between concentrations of each

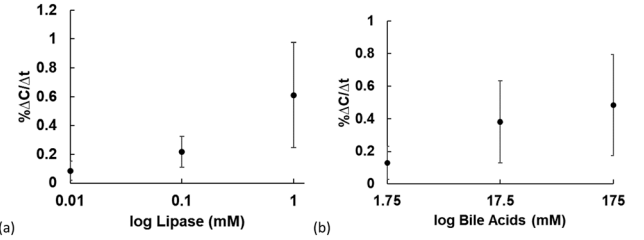

Fig. 7 Semi-logarithmic calibration curves of slope responses for 30 min of (a) PL and (b) BAs (n = 3). X-Axis represents the concentration of the analyte in 40 mL solution under 300 RPM stir at 39 °C. Y-Axis calculated using %Delta;C/(Δt = 30 min). Error bars = standard deviation.

analyte at different magnitudes, indicating a positive correlation between analyte concentration and sensor response within the tested ranges. Statistical analysis was performed, consisting of one-way ANOVA between the three concentrations (α = 0.05) for both PL and BA respectively resulting in p-values of 0.12 and 0.17. Unfortunately, the slope of the response at different concentrations appear to lack distinction, as one can see that the error bars overlap significantly. The sensor is essentially two capacitors in series, one made of the SG film and another made using the layer of solution above, consisting mostly of water. As the SG film dissolves or reacts from the analyte, it becomes thinner and the effect of the water capacitor becomes larger as its distance to the sensor diminishes. The time course over which this occurs is dependent on several factors including the film thickness. The up to 55% variation in the starting film thickness could explain some of the overlap between the measured result at these concentrations.

Enzymatic kinetics remain a complex issue, and the lack of difference between the removal time of the films (as indicated by the change in capacitance per time) could indicate that the enzymes or emulsion agents are saturated at the lower concentrations and simply are not able to remove the film at a higher rate. Furthermore, the major effect leading to a change in capacitance with the film dissolution is the replacement of the SG film (which has a relatively low relative dielectric constant of ~15.9) with water having a relative dielectric constant of 80. Another possible effect is differences in the emulsification and hydrolysis reactions where hydrolysis *via* PL produces glycerol and stearic acid, each of which impact the capacitance of the sensor during the course of the experiment. Alternatively, emulsification does not alter the material chemical composition, merely the particle size and therefore phase properties of the film, allowing enhanced exposure of the SiO_2 surface of the sensors to constituents in the environmental fluid, even those such as divalent cations.[66] However, the fact that the capacitance change curves are similar for the hydrolysis and emulsification reaction indicate that likely in both cases the change in capacitance is likely due to changes in dielectric constant due to water instead of being dominated by the production of an intermediate analyte. Future investigations will need to focus on how to generate a sensor response that is more concentration dependent. Fortunately, a sensor such as the one demonstrated here could find use in GI diagnostic applications where luminal contents are refluxing or failing to be absorbed properly, making it present in a portion of the alimentary canal where it is irritating. Examples of this include bile reflux into the stomach, bile entry into the colon, and acid reflux into the stomach.[67,68]

Morphological differences comparing the impact of each species on the SG films, were viewed under SEM (110× magnification), after deposition of a carbon coating for conductivity. The films had been incubated under stir condition to each solution, and removed at two time points, 30 minutes and 60 minutes, as shown in Fig. 8. The 30 minute time point was used to correspond the film morphology to the endpoints of the $\%\Delta C/\Delta T$ values used for Fig. 7, while the 60 minute time point was used to determine if any significant changes in the film morphology occurred beyond the used duration. Here, there is little difference between the samples exposed to either PBS or trypsin, whereas the surfaces for PL and BA indicate significant qualitative changes in roughness and crystallization, respectively, though more on crystallization profiles of stearin can be found elsewhere.[69] For the PL-exposed sample, the surface appears significantly smoother, likely an effect of the hydrolytic interface occurring between PL and the stearin that reduces surface roughness, and therefore interfacial surface area, until eventual saturation. The BA-exposed sample, however, presents the formation of an increasingly fragmented stearin surface, offering insight as to how hydrolysis and emulsification manifest differently on the substrate. Based on the capacitive changes observed in Fig. 6, these structural changes may be direct indicators for changes in either dielectric properties of the film material or, more likely, changes in film thickness through hydrolytic- or emulsification-induced fragmentation, exposing the surface area of the underlying electrodes to the high-dielectric behavior of the buffer. The lack of significant change between the 30 and 60 minute time points also imply that the durations used for the data in Fig. 7 are enough to correspond signal saturation to the morphological state.

Finally, the ability to measure PL within the capsule was tested in benchtop environment that varied the pH overtime and introduced PL at a recorded time point to simulate traveling through the GI tract and detection in the duodenum environment. Fig. 9 presents the result of testing the coated capsule containing the SG-SPAs for performing pH-targeted sampling, using the experiments for Fig. 6 and 7 as reference to determine differences in performance when the sensors are outside of or inside the capsule. The respective conditions are labeled as acid, neutral, and lipase, where the capsule was inserted into a pH 3 solution (0.1 M acetic acid) to represent acidic contents for the stomach, pH 7.3 solution (0.1 M PBS) for the duodenum, and addition of PL (1 mM PL in 0.1 M PBS) as a target analyte, respectively. Here, the

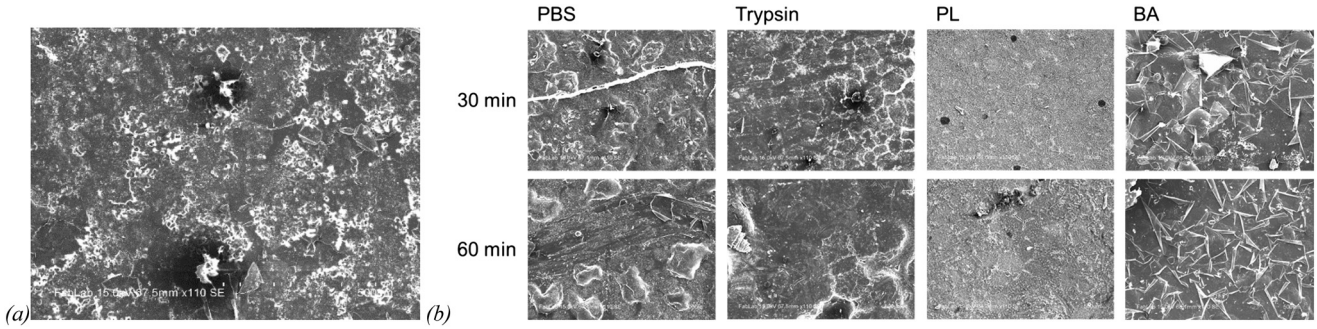

Fig. 8 SEM characterization of SG films at (a) 0 minutes and (b) after exposure to various solutions at 30 and 60 minute time intervals.

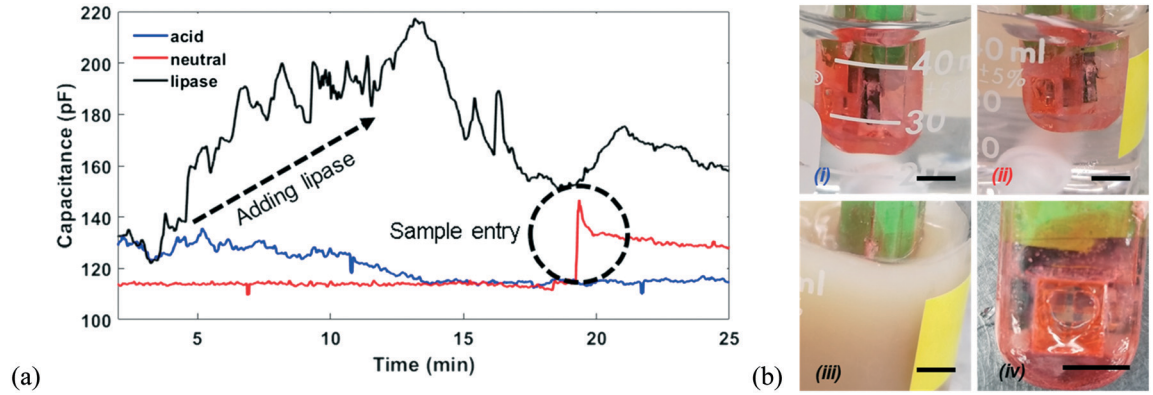

Fig. 9 (a) Combined pH sampling and enzyme sensing in integrated capsule. Measurements were initiated after immersion into acidic solution for 25 minutes (blue), after which the capsules were removed and immersed into a neutral solution (red), where a spike was observed around 19 minutes, indicated by the circle. Finally, the capsule was removed and immersed into a solution containing 1 mM lipase (black), where a distinct increase in capacitance is observed, indicated by the arrow. (b) Photographs taken of the capsule at the end of each respective sequence, designated by the label color: b-i: acid condition, b-ii: neutral condition, b-iii: lipase condition, and b-iv lipase condition after removal from the solution. Scale bar = 5 mm.

sensor responses are overlaid for more direct sequence comparison and presented in capacitance rather than $\%\Delta C$ to show how they compare from beginning to end of each condition. Upon insertion into the acid condition, negative drift was observed from ~129.5 ± 0.772 pF, eventually saturating at 115.2 ± 0.759 pF, though no inflow of solution into the capsule was evident through visual inspection and the color of the buffer solution remained clear as indicated in Fig. 9b-i.[49] After ~19 minutes of incubation in the neutral condition (0.1 M PBS), a distinct increase in capacitance to 146.1 pF was observed, before reaching saturation at 127.9 ± 0.433 pF. Additionally, the color of the solution gained a red hue reflective of the Eudragit L100 coating color, as seen in Fig. 9b-ii, indicating sample entry. Once the capsule was inserted into the lipase condition, there was an immediate effect similar to the capacitance sequences observed in Fig. 6a, where there is a rapid increase in capacitance over ~14 minutes to reach 216.0 ± 0.602 pF, or 66.8% increase from the beginning, with some signal fluctuation and decrease as well until it levels around 158.5 ± 0.913 pF, or a 22.4% increase. Due to the opacity of the PL solution, no distinguishable features were discernable until capsule removal, where there is a noticeable region in the Eudragit L100 coating where the fluid could enter the capsule sensing chamber, shown in Fig. 9b-iv.

The slope from the first 30 minutes of the lipase condition was calculated to yield 0.198 pF min^{-1}. Comparing the linear fit with that produced in Fig. 7a, the slope changes with concentration of PL. This slope is calculated as a ~3-fold loss in sensor response compared to the mean response for 1 mM lipase (0.610 ± 0.364 pF min^{-1}) while also outside the error range, indicating potential loss in SG-SPA response to the analyte when packaged within the capsule rather than when tested without it; this is not surprising, though, considering the differences in fluid dynamics and flow profile of the analyte in the sensing chamber as opposed to when the SG-SPA is surrounded by the fluid in the beaker. However, this emphasizes the need to enhance the exposure of the SG-coated sensors to the surrounding environment, which can be implemented by reducing the thickness of the 3D-printed shell at the inlets or by embedding the sensors directly onto the outermost packaging of the capsule. Ultimately, this experiment demonstrated the sequential ability of the capsule package to remain intact in a potential gastric

environment, dissolve from duodenal fluids and allow detection of PL in the same environment. Based on the results presented in Fig. 6 and 7, it is likely this similar strategy can be leveraged to detect BAs in target pH environments as well, in addition to measuring PL or BA related pathologies such as those discussed above.

Conclusion

This work presents a proof-of-concept demonstration of triglyceride-based coatings for monitoring simulated duodenal analytes in an integrated capsule system. The contents consist of preliminary sensor characterization while primarily introducing a system-integrated approach to ingestible device packaging and the potentials for a novel sensing platform for lipase and bile acids. The device discussed in this paper demonstrates the ability to measure and wirelessly transmit changes in capacitance due to both film hydrolysis and emulsification reactions as a result of exposure of stearin films to PL and BAs, respectively. For PL, signals were measurable for 10 μM–1 mM concentrations, whereas signals from BAs were distinguishable between 1.75–175 mM concentrations, each of which are within physiologically relevant ranges for healthy and abnormal levels. For each concentration, the observed slope produced from the first 30 minutes, which is well within the average duration range for material traveling through the human duodenum, was usable to relate the signal to its respective concentration.[64] Furthermore, morphological differences were characterized in triglyceride-based films after exposure to various duodenal contents, giving insight as to the physical manifestation of hydrolytic *versus* emulsification reaction mechanism. Finally, the ability to detect PL after subsequent targeting at a pH-specific environment was demonstrated, and it was found that the design of the sensing chamber and the respective inlets could be thinned to prevent reduction in the reactive interface between the sensor surface and environmental contents.

While sensor characterization was limited to environments that only simulated duodenal fluids in pH and isolated analytes, rather than *in vivo* systems, there remain several limitations to our methods for signal analysis and the platform in general. For example, parametric analyses of slopes over different time intervals may allow for distinguishing between each film response over time, thus producing more sensitive or optimal fitting equations to match the concentration with the $\%\Delta C/\Delta T$. The sensor responses are also likely to increase sensitivity if thinner insulating films can be deposited; this would change the amount of substrate and therefore amount of reaction that needs to occur to increase the rate of change in dielectric mismatch between the film and environmental solution, potential altering resulting concentration range for other GI regions where it may be relevant. Next, each species was tested in isolation, and their simultaneous presence has been shown to reduce efficacy due to non-specific film interactions depending on the material used.[28] Therefore, it is critical that future work will focus on characterizing and optimizing the sensor performance over a wider concentration range, adding more non-specific species to determine further reaction specificity, and incorporate additional food-based materials, such as gelatin – substrates for monitoring other types of pancreatic enzymes.[28] Additionally, different capsule coating materials could be used toward measuring these species in different GI environments – based on their pH – as well as enhance the exposure of the substrate to materials in the external environment. The coatings can be used to protect and expose different types of biosensors to their target regions, enhancing passive localization strategies while notifying the system user of the exact time of exposure. On a similar note, while stearin has demonstrated the potential utility as a substrate for measuring time dependency of either hydrolytic or emulsification reactions, more control over testing conditions would reduce sources of electrical or environmental noise or impedance sensing could be used to examine additional electrical properties of the films. This includes improving the coating process for producing more consistent SG film thicknesses, improving the starting conditions for each of the sensors. Further investigation is needed of strategies for imparting control to the system or over environmental features to improve analysis since these systems are directed to function in the GI tract, which is an inherently chaotic environment.

Ultimately, this platform provides opportunities for sensing hydrolytic and emulsification reactions, such as through other enzymes or biologicals similar to the species discussed in this work, along with an innovative packaging strategy toward passive GI targeting in minimally invasive and ingestible diagnostics.

Conflicts of interest

There are no conflicts to declare.

Acknowledgements

This work was supported by the National Science Foundation ECCS Program under Award 1738211. The authors acknowledge the support from the Maryland NanoCenter and its FabLab.

References

1 L. A. Beardslee, G. E. Banis, S. Chu, S. Liu, A. A. Chapin and J. M. Stine, *et al.* Ingestible Sensors and Sensing Systems for Minimally Invasive Diagnosis and Monitoring: The Next Frontier in Minimally Invasive Screening, *ACS Sens.*, 2020, **5**(4), 891–910.

2 K. Kalantar-zadeh, N. Ha, J. Z. Ou and K. J. Berean, Ingestible Sensors, *ACS Sens.*, 2017, **2**(4), 468–483, DOI: 10.1021/acssensors.7b00045.

3 J. L. Gonzalez-Guillaumin, D. C. Sadowski, K. V. I. S. Kaler and M. P. Mintchev, Ingestible Capsule for Impedance and pH Monitoring in the Esophagus, *IEEE Trans. Biomed. Eng.*, 2007, **54**(12), 2231–2236.

4 M. R. Basar, F. Malek, K. M. Juni, M. S. Idris and M. I. M. Saleh, Ingestible Wireless Capsule Technology: A Review of Development and Future Indication, *Int. J. Antenn. Propag.*, 2012, **2012**, 807165, DOI: 10.1155/2012/807165.

5 A. Nemeth, D. Agardh, G. Wurm Johansson, H. Thorlacius and E. Toth, Video capsule endoscopy in pediatric patients with Crohn's disease: a single-center experience of 180 procedures, *Ther. Adv. Gastroenterol.*, 2018, **11**, 1756284818758929, Available from: http://www.ncbi.nlm.nih.gov/pubmed/29531578.

6 D. Friedel, R. Modayil and S. Stavropoulos, Colon Capsule Endoscopy: Review and Perspectives, *Gastroenterol. Res. Pract.*, 2016, **2016**, 9643162, Available from: http://www.ncbi.nlm.nih.gov/pmc/articles/PMC5028851/.

7 S. N. Adler and Y. C. Metzger, PillCam COLON capsule endoscopy: recent advances and new insights, *Ther. Adv. Gastroenterol.*, 2011, **4**(4), 265–268, Available from: http://www.ncbi.nlm.nih.gov/pmc/articles/PMC3131168/.

8 A. Moglia, A. Menciassi, P. Dario and A. Cuschieri, Capsule endoscopy: progress update and challenges ahead, *Nat. Rev. Gastroenterol. Hepatol.*, 2009, **6**(6), 353–361, Available from: http://www.nature.com/articles/nrgastro.2009.69.

9 J. Z. Ou, J. J. Cottrell, N. Ha, N. Pillai, C. K. Yao and K. J. Berean, *et al.* Potential of in vivo real-time gastric gas profiling: a pilot evaluation of heat-stress and modulating dietary cinnamon effect in an animal model, *Sci. Rep.*, 2016, **6**, 33387, DOI: 10.1038/srep33387.

10 K. Kalantar-zadeh, C. K. Yao, K. J. Berean, N. Ha, J. Z. Ou and S. A. Ward, *et al.* Intestinal Gas Capsules: A Proof-of-Concept Demonstration, *Gastroenterology*, 2015, **150**(1), 37–39, DOI: 10.1053/j.gastro.2015.07.072.

11 J. Z. Ou, C. K. Yao, A. Rotbart, J. G. Muir, P. R. Gibson and K. Kalantar-zadeh, Human intestinal gas measurement systems: in vitro fermentation and gas capsules, *Trends Biotechnol.*, 2015, **33**(4), 208–213, Available from: http://www.sciencedirect.com/science/article/pii/S0167779915000256.

12 K. Kalantar-Zadeh, K. J. Berean, N. Ha, A. F. Chrimes, K. Xu and D. Grando, *et al.* A human pilot trial of ingestible electronic capsules capable of sensing different gases in the gut, *Nat. Electron.*, 2018, **1**(1), 79–87, Available from: http://www.nature.com/articles/s41928-017-0004-x.

13 P. J. Van Der Schaar, J. F. Dijksman, H. Broekhuizen-De Gast, J. Shimizu, N. Van Lelyveld and H. Zou, *et al.* A novel ingestible electronic drug delivery and monitoring device, *Gastrointest. Endosc*, 2013, **78**(3), 520–528, DOI: 10.1016/j.gie.2013.03.170.

14 W. Yu, R. Rahimi, M. Ochoa, R. Pinal and B. Ziaie, A Smart Capsule With GI-Tract-Location-Specific Payload Release, *IEEE Trans. Biomed. Eng.*, 2015, **62**(9), 2289–2295, Available from: http://ieeexplore.ieee.org/document/7089218/.

15 Q. Shi, J. Wang, D. Chen and J. Chen, In Vitro and In Vivo characterization of wireless and passive micro system enabling gastrointestinal pressure monitoring, *Biomed. Microdevices*, 2014, 859–868.

16 M. S. Arefin, J.-M. Redoute and M. R. Yuce, Integration of Low-Power ASIC and MEMS Sensors for Monitoring Gastrointestinal Tract Using a Wireless Capsule System, *IEEE J. Biomed. Health Inform.*, 2016, **22**(1), 87–97, Available from: http://ieeexplore.ieee.org/document/7891895/.

17 P. Demosthenous and J. Georgiou, An ingestible, NIR-fluorometric, cancer-screening capsule, in *2015 37th Annual International Conference of the IEEE Engineering in Medicine and Biology Society (EMBC)*, IEEE, 2015, pp. 2143–2146, Available from: http://ieeexplore.ieee.org/document/7318813/.

18 A. Nemiroski, M. Ryou, C. Thompson and R. Westervelt, Swallowable Fluorometric Capsule for Wireless Triage of Gastrointestinal Bleeding, *Lab Chip*, 2015, **15**, 4479–4487, Available from: http://pubs.rsc.org/en/Content/ArticleLanding/2015/LC/C5LC00770D.

19 M. Mimee, P. Nadeau, A. Hayward, S. Carim, S. Flanagan and L. Jerger, *et al.* An ingestible bacterial-electronic system to monitor gastrointestinal health, *Science*, 2018, **360**(6391), 915–918, Available from: http://www.ncbi.nlm.nih.gov/pubmed/29798884.

20 A. F. P. van Putten, *Electronic Measurement Systems*, Routledge, 2019, Available from: https://www.taylorfrancis.com/books/9781351453141.

21 H. M. Said and F. K. Ghishan, *Physiology of the gastrointestinal tract*, 2018, p. 24.

22 H. N. Chan, M. J. A. Tan and H. Wu, Point-of-care testing: applications of 3D printing, *Lab Chip*, 2017, **17**, 2713–2739, DOI: 10.1039/C7LC00397H.

23 K. Tappa and U. Jammalamadaka, Novel Biomaterials Used in Medical 3D Printing Techniques, *J. Funct. Biomater.*, 2018, **9**(1), 17, Available from: https://www.ncbi.nlm.nih.gov/pubmed/29414913.

24 H. N. Chia and B. M. Wu, Recent advances in 3D printing of biomaterials, *J. Biol. Eng.*, 2015, **9**, 4, DOI: 10.1186/s13036-015-0001-4.

25 W. Jamróz, J. Szafraniec, M. Kurek and R. Jachowicz, 3D Printing in Pharmaceutical and Medical Applications - Recent Achievements and Challenges, *Pharm. Res.*, 2018, **35**(9), 176, Available from: https://www.ncbi.nlm.nih.gov/pubmed/29998405.

26 R. D. Sochol, E. Sweet, C. C. Glick, S.-Y. Wu, C. Yang and M. Restaino, *et al.* 3D printed microfluidics and microelectronics, *Microelectron. Eng.*, 2018, **189**, 52–68, Available from: https://www.sciencedirect.com/science/article/pii/S0167931717304070.

27 W. Xu, H. Yang, W. Zeng, T. Houghton, X. Wang and R. Murthy, *et al.* Food-Based Edible and Nutritive Electronics, *Adv. Mater. Technol.*, 2017, **2**(11), 1700181, DOI: 10.1002/admt.201700181.

28 G. Banis, A. L. Beardslee and R. Ghodssi, Gelatin-Enabled Microsensor for Pancreatic Trypsin Sensing, *Appl. Sci.*, 2018, **8**, 208.

29 M. Stoytcheva, R. Zlatev, Z. Velkova and G. Montero, Nanoparticle modified QCM-based sensor for lipase activity determination, *Anal. Methods*, 2013, **5**(16), 3811–3815, DOI: 10.1039/C3AY41047A.

30 M. Stoytcheva, R. Zlatev, S. Cosnier, M. Arredondo and B. Valdez, High sensitive trypsin activity evaluation applying a nanostructured QCM-sensor, *Biosens. Bioelectron.*, 2013, **41**(1), 862–866, DOI: 10.1016/j.bios.2012.08.039.

31 J. Kim, I. Jeerapan, B. Ciui, M. C. Hartel, A. Martin and J. Wang, Edible Electrochemistry: Food Materials Based Electrochemical Sensors, *Adv. Healthcare Mater.*, 2017, **6**(22), 1700770, DOI: 10.1002/adhm.201700770.

32 S. J. Pandol, *The Exocrine Pancreas*, Morgan Claypool Life Sci, 2010, Available from: https://www.ncbi.nlm.nih.gov/books/NBK54128/.

33 M. Koziolek, M. Grimm, D. Becker, V. Iordanov, H. Zou and J. Shimizu, *et al.* Investigation of pH and Temperature Profiles in the GI Tract of Fasted Human Subjects Using the Intellicap® System, *J. Pharm. Sci.*, 2015, **104**(9), 2855–2863, Available from: http://www.sciencedirect.com/science/article/pii/S002235491630065X.

34 G. E. Banis, L. A. Beardslee, J. M. Stine, R. M. Sathyam and R. Ghodssi, Gastrointestinal Targeted Sampling and Sensing via Embedded Packaging of Integrated Capsule System, *J. Microelectromech. Syst.*, 2019, 1–7, Available from: https://ieeexplore.ieee.org/document/8643033/.

35 E. T. Cole, R. A. Scott, A. L. Connor, I. R. Wilding, H. U. Petereit and C. Schminke, *et al.* Enteric coated HPMC capsules designed to achieve intestinal targeting, *Int. J. Pharm.*, 2002, **231**(1), 83–95.

36 V. Ruiz-Valdepeñas Montiel, J. R. Sempionatto, B. Esteban-Fernández de Ávila, A. Whitworth, S. Campuzano and J. M. Pingarrón, *et al.* Delayed Sensor Activation Based on Transient Coatings: Biofouling Protection in Complex Biofluids, *J. Am. Chem. Soc.*, 2018, **140**(43), 14050–14053, DOI: 10.1021/jacs.8b08894.

37 V. Ruiz-Valdepeñas Montiel, J. R. Sempionatto, S. Campuzano, J. M. Pingarrón, B. Esteban Fernández de Ávila and J. Wang, Direct electrochemical biosensing in gastrointestinal fluids, *Anal. Bioanal. Chem.*, 2018, 1–8, DOI: 10.1007/s00216-018-1528-2.

38 M. E. Haupt, M. J. Kwasny, M. S. Schechter and S. A. McColley, Pancreatic Enzyme Replacement Therapy Dosing and Nutritional Outcomes in Children with Cystic Fibrosis, *J. Pediatr.*, 2014, **164**(5), 1110–1115.e1, Available from: http://www.sciencedirect.com/science/article/pii/S0022347614000286.

39 H. Harada, A. Ono, N. Yamamoto, I. Ikubo, A. Negron and T. Hayashi, *et al.* Studies on Human Pure Pancreatic Juice Collected by Endoscopic Retrograde Catheterization of the Papilla, *Gastroenterol. Jpn.*, 1978, **13**(5), 383–389.

40 E. K. Ulleberg, I. Comi, H. Holm, E. B. Herud, M. Jacobsen and G. E. Vegarud, Human Gastrointestinal Juices Intended for Use in In Vitro Digestion Models, *Food Dig.*, 2011, **2**(1–3), 52–61, Available from: http://www.ncbi.nlm.nih.gov/pmc/articles/PMC3339592/.

41 D. M. Goldberg and K. G. Wormsley, The interrelationships of pancreatic enzymes in human duodenal aspirate, *Gut*, 1970, **11**(10), 859–866, Available from: http://www.ncbi.nlm.nih.gov/pmc/articles/PMC1553158/.

42 M. Raimondo, M. Imoto and E. P. Dimagno, Rapid endoscopic secretin stimulation test and discrimination of chronic pancreatitis and pancreatic cancer from disease controls, *Clin. Gastroenterol. Hepatol.*, 2003, **1**(5), 397–403, Available from: http://www.sciencedirect.com/science/article/pii/S1542356503001824.

43 *Lipase*, Available from: https://labtestsonline.org/tests/lipase.

44 G. J. Kost, Guidelines for point-of-care testing. Improving patient outcomes, *Am. J. Clin. Pathol.*, 1995, **104**(4 Suppl 1), S111–S127, Available from: http://www.ncbi.nlm.nih.gov/pubmed/7484942.

45 P. Vijayvargiya, M. Camilleri and A. Shin, Saenger A. Methods for diagnosis of bile acid malabsorption in clinical practice, *Clin. Gastroenterol. Hepatol.*, 2013, **11**(10), 1232–1239, Available from: http://www.ncbi.nlm.nih.gov/pubmed/23644387.

46 C. Degirolamo, S. Modica, G. Palasciano and A. Moschetta, Bile acids and colon cancer: Solving the puzzle with nuclear receptors, *Trends Mol. Med.*, 2011, **17**(10), 564–572, Available from: https://www.sciencedirect.com/science/article/pii/S1471491411000979?via%3Dihub#bib0190.

47 K. Cheng and J.-P. Raufman, Bile acid-induced proliferation of a human colon cancer cell line is mediated by transactivation of epidermal growth factor receptors, *Biochem. Pharmacol.*, 2005, **70**(7), 1035–1047, Available from: https://www.sciencedirect.com/science/article/pii/S0006295205004612.

48 L. Wedlake, R. A'Hern, D. Russell, K. Thomas, J. R. F. Walters and H. J. N. Andreyev, Systematic review: the prevalence of idiopathic bile acid malabsorption as diagnosed by SeHCAT scanning in patients with diarrhoea-predominant irritable bowel syndrome, *Aliment. Pharmacol. Ther.*, 2009, **30**(7), 707–717, DOI: 10.1111/j.1365-2036.2009.04081.x.

49 G. E. Banis, S. Member, L. A. Beardslee, J. M. Stine, R. M. Sathyam and R. Ghodssi, Gastrointestinal Targeted Sampling and Sensing via Embedded Packaging of Integrated Capsule System, *J. Microelectromech. Syst.*, 2019, 1–7.

50 A. Koulaouzidis, Wireless endoscopy in 2020: Will it still be a capsule?, *World J. Gastroenterol.*, 2015, **21**(17), 5119, Available from: http://www.wjgnet.com/1007-9327/full/v21/i17/5119.htm.

51 G. H. Charbonnet and W. S. Singleton, Thermal properties of fats and oils, *J. Am. Oil Chem. Soc.*, 1947, **24**(5), 140–142, DOI: 10.1007/BF02643296.

52 G. Lake-Bakaar, S. McKavanagh, C. E. Rubio, O. Epstein and J. A. Summerfield, Measurement of trypsin in duodenal juice by radioimmunoassay, *Gut*, 1980, **21**(5), 402–407, Available from: http://www.ncbi.nlm.nih.gov/pubmed/7429303.

53 American Chemical Society, *Reagent chemicals: American Chemical Society specifications, official from April 1, 1993*, The Society, 1993, p. 806.

54 American Society of Biological Chemists, Rockefeller Institute for Medical Research., American Society for Biochemistry and Molecular Biology, *J. Biol. Chem.*, 1938, **123**(3), 679, Available from: http://www.jbc.org/cgi/framedreprint/123/3/679.

55 A. Robles Medina, L. Esteban Cerdán, A. Giménez Giménez, B. Camacho Páez, M. J. Ibáñez González and E. Molina Grima, Lipase-catalyzed esterification of glycerol and polyunsaturated fatty acids from fish and microalgae oils, *J. Biotechnol.*, 1999, **70**(1–3), 379–391, Available from: https://www.sciencedirect.com/science/article/pii/S0168165699000917.

56 P. Speranza, A. P. B. Ribeiro and G. A. Macedo, Lipase catalyzed interesterification of Amazonian patauá oil and palm stearin for preparation of specific-structured oils, *J. Food Sci. Technol.*, 2015, **52**(12), 8268–8275, Available from: http://www.ncbi.nlm.nih.gov/pubmed/26604403.

57 Y. K. Lee, K. J. Yu, Y. Kim, Y. Yoon, Z. Xie and E. Song, *et al.* Kinetics and Chemistry of Hydrolysis of Ultrathin, Thermally Grown Layers of Silicon Oxide as Biofluid Barriers in Flexible Electronic Systems, *ACS Appl. Mater. Interfaces*, 2017, **9**(49), 42633–42638, DOI: 10.1021/acsami.7b15302.

58 D. Bonn, Wetting transitions, *Curr. Opin. Colloid Interface Sci.*, 2001, **6**(1), 22–27, Available from: https://www.sciencedirect.com/science/article/pii/S1359029400000832.

59 M.-C. Michalski and B. J. V. Saramago, Static and Dynamic Wetting Behavior of Triglycerides on Solid Surfaces, *J. Colloid Interface Sci.*, 2000, **227**(2), 380–389, Available from: https://www.sciencedirect.com/science/article/pii/S0021979700968693?via%3Dihub.

60 L. D. A. Chumpitaz, L. F. Coutinho and A. J. A. Meirelles, Surface tension of fatty acids and triglycerides, *J. Am. Oil Chem. Soc.*, 1999, **76**(3), 379–382, DOI: 10.1007/s11746-999-0245-6.

61 W. Xie, W. M. Lewis, J. Kaser, C. Ross Welch, P. Li and C. A. Nelson, *et al.* Design and Validation of a Biosensor Implantation Capsule Robot, *J. Biomech. Eng.*, 2017, **139**(8), 081003, DOI: 10.1115/1.4036607.

62 J. Carrère, C. Galabert, J. P. Thouvenot and C. Figarella, Assay of human pancreatic lipase in biological fluids using a non-competitive enzyme immunoassay, *Clin. Chim. Acta*, 1986, **161**(2), 209–219, Available from: http://www.ncbi.nlm.nih.gov/pubmed/3542306.

63 K. E. Barrett and W. F. Ganong, *Ganong's review of medical physiology*, LK - https://umaryland.on.worldcat.org/oclc/779244271. Lange medical book TA - TT -, McGraw-Hill Medical, New York, 24th edn, 2012, Available from: http://accesspharmacy.mhmedical.com/book.aspx?bookid=393.

64 M. Camilleri, L. J. Colemont, S. F. Phillips, M. L. Brown, G. M. Thomforde and N. Chapman, *et al.* Human gastric emptying and colonic filling of solids characterized by a new method, *Am. J. Physiol.*, 1989, **257**(2), G284–G290.

65 Z. Huang, T. Yu, L. Guo, Z. Lin, Z. Zhao and Y. Shen, *et al.* Effects of triglycerides levels in human whole blood on the extraction of 19 commonly used drugs using liquid-liquid extraction and gas chromatography-mass spectrometry, *Toxicol. Rep.*, 2015, **2**, 785–791, Available from: http://www.ncbi.nlm.nih.gov/pubmed/28962414.

66 Y. K. Lee, K. J. Yu, Y. Kim, Y. Yoon, Z. Xie and E. Song, *et al.* Kinetics and Chemistry of Hydrolysis of Ultrathin, Thermally Grown Layers of Silicon Oxide as Biofluid Barriers in Flexible Electronic Systems, *ACS Appl. Mater. Interfaces*, 2017, **9**(49), 42633–42638, DOI: 10.1021/acsami.7b15302.

67 J. J. G. Marin, R. I. R. Macias, O. Briz, J. M. B. Monte and M. J. Monte, Bile Acids in Physiology, Pathology and Pharmacology, *Curr. Drug Metab.*, 2016, **17**, 4–29, Available from: http://www.eurekaselect.com/node/136443/article.

68 W. K. H. Kauer and H. J. Stein, Bile Reflux in the Constellation of Gastroesophageal Reflux Disease, *Thorac. Surg. Clin.*, 2005, **15**(3), 335–340, Available from: http://www.sciencedirect.com/science/article/pii/S1547412705000186.

69 W. Jiao, L. Li, A. Yu, D. Zhao, B. Sheng and M. Aikelamu, *et al.* In Vitro Gastrointestinal Digestibility of Crystalline Oil-in-Water Emulsions: Influence of Fat Crystal Structure, *J. Agric. Food Chem.*, 2019, **67**(3), 927–934, DOI: 10.1021/acs.jafc.8b04287.

